Travelling wave magnetic valveless micropump driven by rotating integrated magnetic arrays

Weixiang Ye[1,2], *Wei Zhang*[1,2], *Cheng Wang*[1,2,3], *Wenbin Li*[1,2], *Zhao Yue*[1,2], *Guohua Liu*[1,2]

[1]*College of Electronic Information and Optical Engineering, Nankai University, Tianjin 300071, People's Republic of China*
[2]*Key Laboratory of Photo-electronic Thin Film Devices and Technology of Tianjin, Nankai University, Tianjin 300071, People's Republic of China*
[3]*Department of Mechanical Engineering, Columbia University, New York 10027, USA*
E-mail: liugh@nankai.edu.cn

Published in Micro & Nano Letters; Received on 13th January 2014; Revised on 6th March 2014; Accepted on 7th March 2014

A novel magnetic valveless micropump is proposed for microfluidic applications. Two integrated NdFeB permanent magnetic arrays were used to generate a travelling wave on the top wall of the elastic microchannel, and then the liquid particles were transported along with the travelling wave in the microchannel. The characteristics tested at different frequencies demonstrate that the magnetic micropump has a much higher driving efficiency than the piezoelectric micropump with the same saw-toothed microchannel. By using a low power supply (3.7 V $V_{p\text{-}p}$, 185 mW), the magnetic micropump significantly improves the maximum flow rate and back pressure to 184.25 µl/min and 1.28 kPa with the microchannel of 200 µm width.

1. Introduction: The micropump is an essential functional component in a variety of applications, especially for the micrototal analysis system that requires precise manipulation of the liquid on a chip [1–3]. In recent years, there have been numerous reports on developing, modelling and the optimisation of a variety of micropumps [4, 5]. Among them, the valveless micropump has arisen as a particularly attractive choice because of its extended working range, no moving parts, easy fabrication, cost-effectiveness and miniaturisation [6, 7].

Based on the principle of the travelling wave driving mechanism [8, 9], we introduce a novel travelling wave magnetic valveless micropump, which is driven by rotating magnetic arrays. This actuation mechanism performs with a rapid response time and a fairly large interactive force which yields large vibrations on the top wall of the microchannel with low actuating voltage. Without any change of the microchannel, the magnetic micropump has a considerable improvement in maximum flow rate and back pressure compared with the piezoelectric micropump. In addition, the magnetic micropump has great potential for integrated fabrication on a chip because the structure can be simplified and downsized easily.

2. Design and working principle

2.1. Design of micropump: Fig. 1*a* shows an expanded diagram of the structure of the magnetic micropump. From bottom to top, it comprises five parts, namely the lower substrate, microchannel, upper substrate, cylindrical micromagnet array and ring-shaped micromagnet array. The lower substrate was designed to hold the microchannel, the upper substrate above the microchannel was moulded and integrated with the cylindrical micromagnet array. A DC electric minimotor (6 mm in diameter and 14 mm in length) was mounted on the top side of the upper substrate.

Fig. 1*b* presents the cross-sectional view of the magnetic micropump. The saw-toothed microchannel was bonded on the lower substrate and covered by the upper substrate. To generate a travelling wave, the magnet arrays need to be mounted with the proper orientations. Four microcylindrical permanent magnets (2 mm in height and 1 mm in diameter, $B = 500$ Gauss at 1 mm above its surface) with the same magnetic pole orientation were embedded in the upper substrate side by side and in contact with the top wall of each diffuse element of the elastic microchannel. Another four microring-shaped permanent magnets (2 mm in height, 1 mm in inner diameter and 2.3 mm in outer diameter, $B = 800$ Gauss at 1 mm above its surface) were mounted on the rotation shaft of the motor and aligned to the cylindrical magnets one by one. The magnetic pole orientation of ring-shaped magnets were arranged with successively descending $\pi/2$rad. The gap between the ring-shaped magnets and the upper substrate is $d_1 = 0.8$ mm, and the interval between adjacent cylindrical magnets is $d_2 = 1$ mm.

For a convictive crosswise comparison between the magnetic micropump and the piezoelectric micropump, the saw-toothed microchannel is exactly the same as our previous work [9], as shown in Fig. 2*a*. The size parameters of each diffuse element are

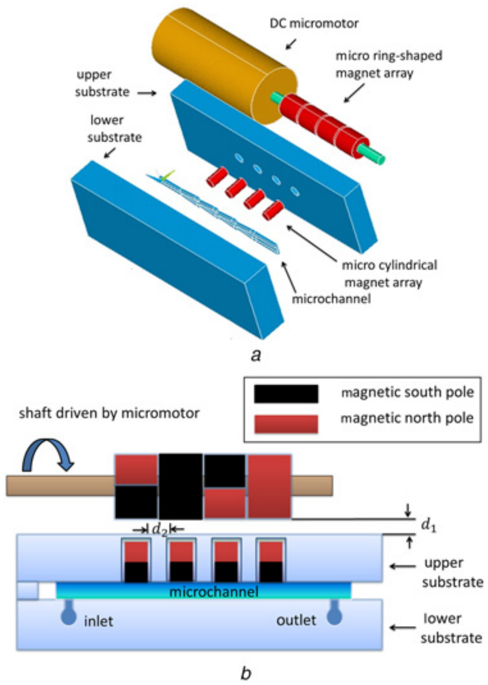

Figure 1 *Diagram of travelling wave magnetic valveless micropump*
a Three-dimensional (3D) components schematic
b Cross-sectional view

doi: 10.1049/mnl.2014.0022

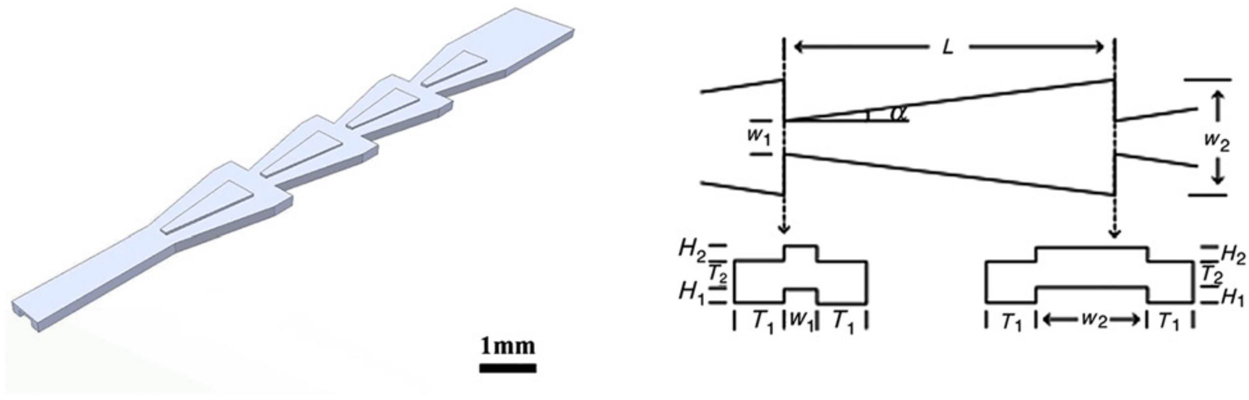

a

b

Figure 2 *Configuration of saw-toothed microchannel*
a 3D structure of saw-toothed microchannel
b Configuration of diffuse elements

$\alpha = 6.5°$, $W_1 = 200$ µm, $W_2 = 700$ µm, $L = 2.1$ mm, $H_1 = 100$ µm, $H_2 = 100$ µm, $T_1 = 300$ µm and $T_2 = 200$ µm, as shown in Fig. 2*b*.

The microchannel was fabricated by polydimethylsiloxane (PDMS) moulding technology which was reported in our previous work with minor modification [9]. The upper and lower substrates were made of polymethylmethacrylate (PMMA) slabs by using a circuit board plotter (ProtoMat H100, LPKF, Germany). Firstly, the mixture of PDMS base and curing agent (volume ratio of 11:1) was injected to the PMMA moulds after degassing in the relative vacuum of −1 kg/cm^2 pressure, and cured at 50°C for about 50 min. Afterwards, the microchannel is finished after stripping from the mould and bonding to the lower substrate at 55°C for 1 h. Finally, the cylindrical micromagnet array was embedded in the upper substrate, while the minimotor was mounted on the top side of the upper substrate. The motor was driven by programmable pulse-width modulation square waveforms ($V_{\text{p-p}} = 3.7$ V), which were generated by a MSP430 microcontroller circuitry. The entire setup of the magnetic micropump and the drive circuitry are shown in Figs. 3*a* and *b*.

2.2. Principle of actuation: The travelling wave magnetic valveless micropump is a novel microfluidic driving technique, whose principle is that a travelling wave beneath the top wall of the elastic microchannel was generated by the interactive forces between two integrated magnetic arrays. Then the liquid particles were transported along with the travelling wave in the microchannel. Fig. 4 shows the fluid particles beneath the top wall of the microchannel move forward with the travelling wave because of its viscosity and the periodic variation of the local pressure. The flow rate of the liquid particles can be controlled by changing the magnitude and frequency of the generated travelling wave.

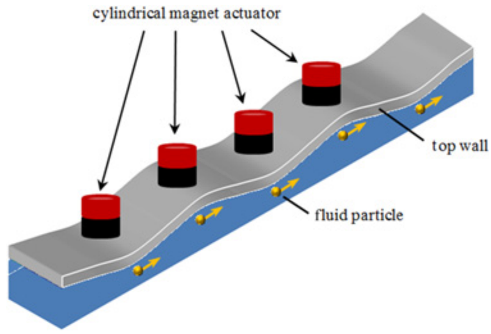

Figure 4 *Driving mechanism of travelling wave magnetic valveless micropump*

The travelling wave beneath the top wall can be generated by the proper magnetic pole orientation arrangement of these two magnet's arrays. In Fig. 1, the cylindrical magnet actuators are arranged with the same magnetic pole orientation and the ring-shaped magnets are arranged with the magnetic pole orientation with successively descending $\pi/2$rad. During one rotation cycle of the motor, four cylindrical magnet actuators generate four standing waves with the same amplitude, and with $\pi/2$rad phase differences, respectively. Assuming any two standing waves generated by adjacent magnet actuators as A and B, they can be expressed as the following equations

$$y_A = \varepsilon_0 \cdot \sin\frac{2\pi x}{\lambda} \cdot \sin\omega_0 t \quad (1)$$

$$y_B = \varepsilon_0 \cdot \cos\frac{2\pi x}{\lambda} \cdot \cos\omega_0 t \quad (2)$$

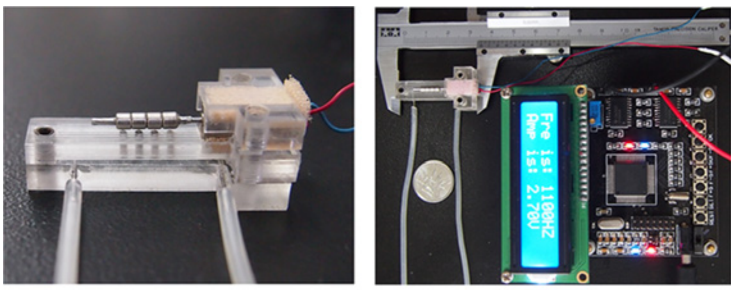

a *b*

Figure 3 *Physical image of travelling wave magnetic valveless micropump and drive circuitry*
a Micropump
b Entire setup of the magnetic micropump

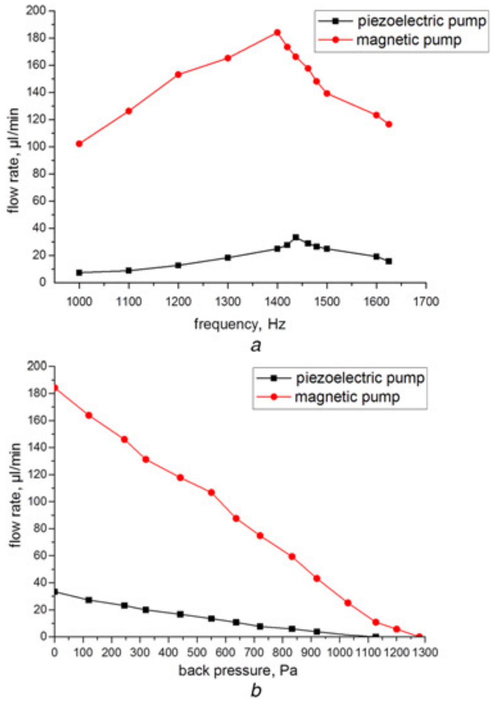

Figure 5 *Experimental results*
a Curve of average flow rates
b Curve of flow rates against back pressures

Combining (1) and (2)

$$y = y_A + y_B = \varepsilon_0 \times \cos\left(\frac{2\pi}{\lambda} - \omega_0 t\right) \qquad (3)$$

Equation (3) illustrates that the travelling wave can be generated by two standing waves with the same amplitude, the same frequency and the $\pi/2$rad phase differences and the magnetic micropump can work with at least two microcylindrical magnets and two microring-shaped magnets. Our experiments also prove that it can work successfully with two magnets. However, for the sake of improving the driving capacity and efficiency, the magnetic arrays with four magnets were adopted in the following experiments.

3. Experiments and discussion: The characteristics of the magnetic micropump can be easily controlled by simply changing the rotation speed of the motor. We tested the flow rates at driving frequencies ranged from 1 to 1.6 kHz, which corresponds to the rotation speed of the motor from 15 000 to 24 000 rpm roughly and we also measured the back pressures by observing the liquid level heights of the micropump's outlet at different flow rates. For a reference, a piezoelectric micropump with the same saw-toothed microchannel, which had been reported in our previous Letter [9], has also been tested in the same driving frequency range.

The average flow rates for deionised water at different frequencies of the magnetic micropump and piezoelectric micropump are given in Fig. 5*a*. The inverse proportion between the average flow rates and the back pressures are shown in Fig. 5*b*. The magnetic micropump reaches the maximum flow rate and back pressure (184.25 µl/min and 1.28 kPa) at 1400 Hz (motor rotation speed is 21 000 rpm). By comparison, the piezoelectric micropump provides the maximum flow rate and back pressure (33.36 µl/min and 1.13 kPa) at a little higher frequency of 1437 Hz. The corresponding frequency of maximum flow rates and back pressures of these two micropumps are all about 1400 Hz. The average flow rates declined rapidly at the both sides of the maximum, which is in correspondence with the principle of the travelling wave micropump [10]. It implies that only a certain frequency of the driving signal, which depends on the mechanical properties of the PDMS materials, can induce a travelling wave on the microchannel efficiently and for the same microchannel parameters and structure, it is noted that the magnetic micropump has much higher flow rate and back pressure than the piezoelectric micropump. This is because the piezoelectric driving method requires a high actuating voltage to obtain enough driving force, and the driving efficiency of the micropump dropped remarkably with the piezoelectric bimorph array downsizing and low actuating voltage input. Although the magnetic driving method could also provide large magnetic driving forces when there is low actuating voltage input. Meanwhile, the fairly large interactive forces and rapid response time between the two integrated magnetic arrays yield large vibrations on the top wall of the elastic microchannel, which could induce a travelling wave more efficiently in the microchannel.

4. Conclusion: In summary, we have designed and fabricated a novel travelling wave magnetic valveless micropump actuated by the interactive forces between two integrated magnetic arrays. The actuation mechanism of the magnetic micropump has been discussed. Compared with the piezoelectric micropump, the magnetic micropump exhibits a much higher flow rate and back pressure because of the large interactive force and rapid response time between two integrated magnetic arrays. The magnetic micropump can be easily and inexpensively produced by using conventional MEMS techniques and can be further simplified and optimised. It is reasonable to expect that the magnetic micropump with the advantages of low power consumption, high flow rate, simple structure and miniaturisation can be widely utilised in miniaturised and integrated sensing devices.

5. Acknowledgments: This work was supported by the National Natural Science Foundation of China (61271099), the Natural Science Foundation of Tianjin (12JCZDJC20400) and the National Research Foundation for Doctoral Program of Higher Education of China (20120031110031).

6 References

[1] Huikko K., Kostiainen R., Kotiaho T.: 'Introduction to micro-analytical systems: bioanalytical and pharmaceutical applications', *Eur. J. Pharm. Sci.*, 2003, **20**, (2), pp. 149–171

[2] Wang C., Zhang W., Liu R.P., Wang Y.J., Liu G.H.: 'Time-division self-referencing multichannel spectral SPR sensor without mechanical scanning', *Electron. Lett.*, 2013, **49**, (7), pp. 493–495

[3] Wang C., Liu R., Zhang W., ET AL.: 'Multichannel scan surface plasmon resonance biochip with stationary optics and baseline updating capability', *J. Biomed. Opt.*, 2013, **18**, (11), pp. 110502

[4] Iverson B.D., Garimella S.V.: 'Recent advances in microscale pumping technologies: a review and evaluation', *Microfluidics Nanofluidics*, 2008, **5**, (2), pp. 145–174

[5] Amirouche F., Zhou Y., Johnson T.: 'Current micropump technologies and their biomedical applications', *Microsyst. Technol.*, 2009, **15**, (5), pp. 647–666

[6] Lee C.Y., Chen Z.H.: 'Valveless impedance micropump with integrated magnetic diaphragm', *Biomed. Microdevices*, 2010, **12**, (2), pp. 197–205

[7] Fadl A., Demming S., Zhang Z., Büttgenbach S., Krafczyk M., Meyer D.M.: 'A multifunction and bidirectional valve-less rectification micropump based on bifurcation geometry', *Microfluidics Nanofluidics*, 2010, **9**, (2–3), pp. 267–280

[8] Ogawa J., Kanno I., Kotera H., Wasa K., Suzuki T.: 'Development of liquid pumping devices using vibrating microchannel walls', *Sens. Actuators A, Phys.*, 2009, **152**, (2), pp. 211–218

[9] Zhang W., Wang C., Yue Z., Zhan C.N., Geng W.D., Liu G.H.: 'Travelling-wave piezoelectric micropump with low resistance microchannel', *Electron. Lett.*, 2011, **47**, (19), pp. 1065–1066

[10] Zhang W., Wang C., Yue Z., ET AL.: 'Fabrication and measurement of traveling wave piezoelectric micropump', *Nanotechnol. Precision Eng.*, 2013, **11**, (1), pp. 79–84

doi: 10.1049/mnl.2014.0022